NaK $D^1\Pi$ electric dipole moment measurement by Stark level crossing and $e-f$ mixing spectroscopy

M. Tamanis, M. Auzinsh, I. Klincare, O. Nikolayeva, A. V. Stolyarov,[a] and R. Ferber
Department of Physics, University of Latvia, Riga LV-1586, Latvia

(Received 15 April 1996; accepted 7 November 1996)

The paper presents the first permanent electric dipole moment d_p measurements for NaK $D^1\Pi$ state rovibronic levels. Two different methods were applied to obtain d_p values. Stark effect induced level crossing registered as the changes of fluorescence linear polarization $P(\mathscr{E})$ with external electric field $\mathscr{E}$ yielded from one fit both the electric dipole moment value and the Λ-doubling splitting between e,f substates of an individual rotational state. Another method consisted of obtaining the ratio Δ_{ef}^J/d_p from $\mathscr{E}$-dependence of the forbidden line appearing in fluorescence as a result of $e-f$ Stark mixing, along with direct Δ_{ef}^J measurement by RF – optical double resonance. The respective dipole moment values obtained are 5.9 – 6.4 D for the state $v'=7$, $J'=23$, as well as 4.5 – 4.8 D for $v'=12$, $J'=7$, the typical errors being ca. 12%–20%. The d_p value for the latter state reflects d_p diminution expected due to the admixture of the $d^3\Pi$ state caused by intramolecular interaction. Signal simulation and data fitting have been accomplished using direct Hamiltonian diagonalization accounting for Stark interaction within rotational states $J\pm\Delta J, \Delta J=0,1$ and 2 in the initial, excited and final state. © *1997 American Institute of Physics.* [S0021-9606(97)02106-5]

I. INTRODUCTION

There is interest in determining the permanent electric dipole moment of a molecule since this quantity reflects very sensitively the details of electronic structure. At the same time there is still a lack of information about electric dipole moments for short-lived excited states of diatomic molecules. One of the methods to determine electric dipole moments consists of applying the electric-field-induced analog to the Hanle effect. The electric-field-caused changes in atomic fluorescence polarization were first revealed by Hanle[1] as early as in 1926, very soon after his discovery of magnetic-field-induced fluorescence depolarization, or the ''Hanle effect.''[2] These two phenomena are caused by Stark and Zeeman effects respectively, having their physical origin in removing the degeneracy between coherently excited magnetic sublevels M, being thus called ''zero field electric/magnetic field level crossing,'' see monographs.[3–5] The application of external-field-caused level crossing methods to molecules was proposed by Zare.[6] However, as distinct from widely applied magnetic-field-induced level crossings,[3–5] the pure electric-field level crossing signals in resonance fluorescence, first applied to atoms,[7,8] for molecules have been observed in relatively few works, see Refs. 9–11. For the states with closed electronic shells, such as $A^1\Sigma$ in BaO (Ref. 11) and $B^3\Pi_{0_u^+}$ in I_2,[10] the monotonic ''Stark–Hanle'' (Stark analog of Hanle effect) curves were observed in laser-induced fluorescence (LIF). In these cases it is the second-order Stark effect[12,13] which determines the Stark splitting manifold. This follows directly from the selection rules for the electric-dipole allowed interaction, which connects only the states with different, even or odd, total parity, labelled as $+$ or $-$, respectively. Hence, the first-order perturbation terms are absent in the non-degenerated perturbation approach for the Stark operator

$$\hat{\mathbf{H}}_{\mathbf{St}} = -\mathbf{d_p}\mathscr{E}. \tag{1}$$

This means that the terms linear over electric field strength $\mathscr{E}$ equal zero for a rovibronic level with fixed rotational quantum number J. The appearance of linear over $\mathscr{E}$ terms is possible only in the case when the states, which are interacting due to $\hat{\mathbf{H}}_{\mathbf{St}}$, are so close in energy that it is impossible to use the non-degenerate perturbation theory. This is the case for quasi-degenerate electronic states with $\Lambda \neq 0$. In particular, the $^1\Pi$-state possesses two Λ-doublet components of different total parity, $+$ or $-$, within a rotational state J, see Fig. 1(a). The total parity alternates with J, and another type of label, named the e/f symmetry, is often used, which factors out the $(-1)^J$ J-dependence, thus being a rotation-independent label,[14,15] see Fig. 1(a). The Λ-doublet splitting Δ_{ef}^J caused by electron-rotation interaction, is regularly given by $\Delta_{ef}^J = q[J(J+1)-\Lambda^2]$, where q is the Λ-doubling constant. This leads, as distinct from the $^1\Sigma$ state, to the ''quasi-linear'' Stark effect[13] in the $^1\Pi$ state (see Fig. 1(b)).

A deeper insight into the $^1\Pi$ state Stark effect, including Stark zero-field level crossing, was first given by Klemperer and co-authors[9] and applied to the $(A^1\Pi)$ CS molecule. Further, in a number of works,[16–24] the main attention was paid to the changes in the $^1\Sigma \rightarrow {}^1\Pi \rightarrow {}^1\Sigma$ LIF spectra induced by dc Stark effect mixing of e/f levels. Indeed, due to $\Delta J=0,\pm 1$ and $+\leftrightarrow -$ selection rules,[14,15] see Fig. 1(a), only the (P,R)-doublet emission is allowed at P- or R-type excitation, whereas only Q-singlet emission is allowed at Q-type excitation. If, however, an external electric field is applied, the $+\leftrightarrow -$, or e/f Stark effect mixing in a $^1\Pi$ state with fixed J gives rise to the appearance of a ''forbidden''

[a]Department of Chemistry, Moscow M. Lomonosov State University, Moscow W-234, 119899, Russia.

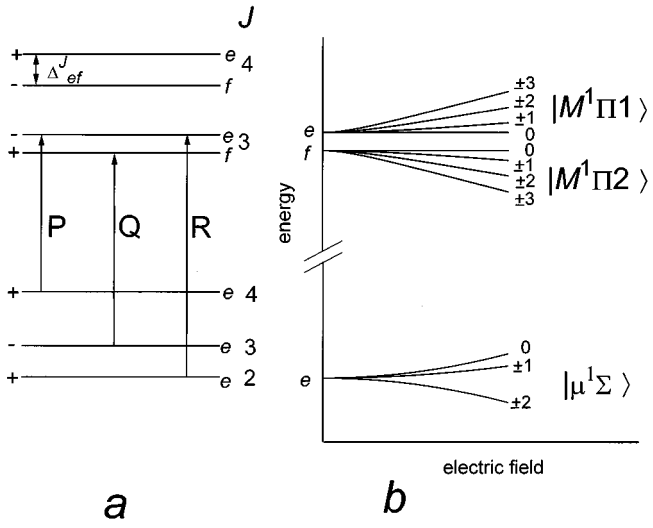

FIG. 1. Selection rules (a) and Stark effect energy shifts (b) for $^1\Sigma - {}^1\Pi$ transition. Notations for (b) refer to Eqs. (4) and (5).

line. Therefore, one can observe in the LIF progression the whole (P,Q,R)-triplet, instead of either doublets or singlets. The relative intensity of a forbidden line, in the case when Δ^J_{ef} is much larger than the natural width of each Λ-doubling component, is mainly governed by the $|(d_p\mathscr{E})/\Delta^J_{ef}|$ parameter, allowing one to obtain the absolute value of d_p, provided additional information on q values can be obtained.

Concerning electronically excited alkali dimers, there have been, according to our knowledge, two attempts to determine d_p, both for NaK $^1\Pi$ states. Drullinger and co-workers[16] have recorded Stark induced ''forbidden'' lines in LIF from NaK $(D^1\Pi)$, and have also demonstrated the RF-optical double resonance signal on the $v'=7, J'=5$ level. However, they present only qualitative information without mentioning any d_p values. Later, Derouard and co-workers[24] made an attempt to determine NaK $(B^1\Pi)$ dipole moments by applying Stark $e-f$ mixing. They present dipole moment values for several vibrational states. These are ca. two times smaller than the values obtained from *ab initio* calculations by Stevens, Konowalow and Ratcliff.[25] In this sense, the predicted[25] large permanent electric dipole moment values, reaching 4.5 D for NaK $(B^1\Pi)$ and 7.8 D for NaK $(D^1\Pi)$ have still not been proved experimentally. It seems, however, that there could be some contradictions within the results given in Ref. 24, manifested in the large discrepancy of q values obtained. Thus, there is still a lack of reliable information about excited state dipole moments even for such a ''test'' alkali dimer as NaK. We also are not aware of such data pertaining to any other alkali dimer. It is important to mention that in Refs. 9,16–24 the description was restricted by the first-order Stark effect, without accounting for Stark mixing of different rotational states, thus the approach used in data processing has to be improved.

The main goals of the present paper are as follows. First, we intend to determine the NaK permanent electric dipole moment values in its $D^1\Pi$ state, for which there exists developed spectroscopic information,[26–32] including lifetime measurements.[33] We have applied two methods: (i) Stark-induced changes in LIF polarization; (ii) Stark induced ''forbidden'' line relative intensity ratio measurements in combination with the direct Δ^J_{ef} measurement by RF-optical double resonance method.[9,34,35] Secondly, we developed further the description of $^1\Pi$-state dc Stark effect, allowing one to calculate the $\mathscr{E}$ dependence of fluorescence intensity for any geometry and polarization type. We used different order perturbation theory, as well as the direct numerical diagonalization of the Hamiltonian matrix accounting for the interaction of rotational states with different J, both in the excited $^1\Pi$ state and in the ground $^1\Sigma$ state. At this point we have not considered the influence of hyperfine effects. In the situation under discussion, the Stark energy remains small with respect to the rotational energy, $d_p\mathscr{E} \ll BJ(J+1)$, which means that the main rotational-vibrational pattern is conserved, as distinct from the ''pendular states'' situation,[36] which takes place for extremely strong electric fields, destroying the rotational motion of a molecule.

The paper starts from the theoretical description of the Stark effect manifestation in $^1\Pi \rightarrow {}^1\Sigma$ fluorescence (Section II). After a quick description of the experiment (Section III), the simulation of expected signals in LIF polarization is given (Section IV), followed by the presentation of experimental results (Section V) and discussion (Section VI).

II. THEORETICAL DESCRIPTION

Let us consider the interaction of cw broad band radiation with diatomic molecules causing a $^1\Pi(v',J') \leftarrow {}^1\Sigma(v'',J'')$ rovibronic transition in the presence of an external static electric field. Using the general density matrix approach,[5,37–39] one may write the density matrix element $f_{MM'}$ of the excited state as

$$ {}^{kl}f_{MM'} = \frac{\tilde{\Gamma}_p}{\Gamma + i^{kl}\Delta\omega_{MM'}} \sum_{\mu} \langle M^1\Pi k|\hat{\mathbf{E}}^*\hat{\mathbf{D}}|\mu^1\Sigma\rangle \times \langle M'^1\Pi l|\hat{\mathbf{E}}^*\hat{\mathbf{D}}|\mu^1\Sigma\rangle^*. \tag{2}$$

Here μ are magnetic sublevels of the ground state $^1\Sigma$ with rotational quantum number J'', whilst M,M' are magnetic sublevels of the excited state with rotational quantum number J', belonging to Λ-doublet components k,l. The unit vector $\hat{\mathbf{E}}$ describes the exciting light polarization, $\hat{\mathbf{D}}$ is the transition dipole moment unit vector, $\tilde{\Gamma}_p$ is the reduced absorption rate, Γ is the effective excited state relaxation rate, ${}^{kl}\Delta\omega_{MM'}$ is the energy splitting between M,M' sublevels, belonging either to the same $(l=k)$ or to the different $(l \neq k)$ Λ-doublet components, accounting both for Λ-doubling and Stark effect level shifts. The excited state density matrix ${}^{kl}f_{MM'}$ allows one to calculate the intensity of fluorescence $I_f(\hat{\mathbf{E}}_\mathbf{f})$ with polarization vector $\hat{\mathbf{E}}_\mathbf{f}$, originating from this state in the transition $J' \rightarrow J''_1$, as

$$I_f(\hat{\mathbf{E}}_\mathbf{f}) = I_0 \sum_{MM'\mu} \sum_{kl} \langle M^1\Pi k|\hat{\mathbf{E}}_\mathbf{f}^*\hat{\mathbf{D}}|\mu^1\Sigma\rangle \times \langle M'^1\Pi l|\hat{\mathbf{E}}_\mathbf{f}^*\hat{\mathbf{D}}|\mu^1\Sigma\rangle^{*kl} f_{MM'}, \quad (3)$$

where I_0 is proportionality coefficient. The structure of Eq. (3) allows one to notice that the terms entering the sums are formed as excited state matrix elements ${}^{kl}f_{MM'}$ multiplied by the observation matrix elements.

The next step is to represent the molecular wave functions in Eqs. (2), (3) accounting for static external electric field effects. Since the external electric field destroys the spherical symmetry, the rotational quantum number J does not remain a good quantum number any more. At the same time the external electric field does not change the axial symmetry, therefore the projection quantum number M (or μ) is still conserved.

The wave functions included in Eqs. (2) and (3) are obtained in a coupled-basis set as expansions over nonperturbed states with different $J_i'(i=e,f)$ and J'' values mixed by the static external electric field. For a $^1\Pi$ excited state we have

$$|M^1\Pi k\rangle = \sum_{J'=1}^{\infty} \sum_{i=e,f} C^k_{\Pi i}(J',M)|J'Mi\rangle, \quad (4)$$

thus obtaining, as it is usually done, a new wave function for each $k=1,2$, found as the linear combination of e and f substates, with mixing coefficients $C^k_{\Pi e}(J',M)$ and $C^k_{\Pi f}(J',M)$.

For the ground electronic state $^1\Sigma$, one can represent the wavefunction $|\mu^1\Sigma\rangle$, by accounting for J''-mixing, as

$$|\mu^1\Sigma\rangle = \sum_{J''=0}^{\infty} C_\Sigma(J'',\mu)|J''\mu\rangle. \quad (5)$$

Coefficients $C_{\Pi i}$ and C_Σ have to be found from diagonalization of the Hamiltonian accounting for molecular rotation and the Stark effect (Eq. (1)).

It is easy to see that the respective matrix elements, both in absorption and fluorescence, are proportional to the multiplication of the correspondent mixing coefficients $C^k_{\Pi i}(J',M)$, and $C_\Sigma(J'',\mu)$ or $C_\Sigma(J_1'',\mu)$. For the absorption, one obtains

$$\langle M^1\Pi k|\hat{\mathbf{E}}^*\hat{\mathbf{D}}|\mu^1\Sigma\rangle = \sum_{J'J''i} C^k_{\Pi i}(J',M)C_\Sigma(J'',\mu) \times \langle J'Mi|\hat{\mathbf{E}}^*\hat{\mathbf{D}}|J''\mu\rangle, \quad (6)$$

and the same for the fluorescence, if one replaces J'' by J_1'' and $\hat{\mathbf{E}}$ by $\hat{\mathbf{E}}_\mathbf{f}$. Eq. (6) allows one to apply the Wigner–Eckart theorem:[5,39–42]

$$\langle J'Mi|\hat{\mathbf{E}}''\hat{\mathbf{D}}|J''\mu\rangle = \sum_q (E^q)^* \frac{1}{\sqrt{2J'+1}} C^{J'M}_{J''\mu 1q}(J',i\|D\|J''), \quad (7)$$

in which, due to the selection rules propagation into the reduced matrix element,[41,42] we have

$$(J',e\|D\|J'') = \begin{cases} \sqrt{G(J',J'')}, & J'-J''=\pm 1 \\ 0, & J'-J''=0,\pm 2,\pm 3,\ldots, \end{cases} \quad (8)$$

$$(J',f\|D\|J'') = \begin{cases} \sqrt{G(J',J'')}, & J'-J''=0, \\ 0, & J'-J''=\pm 1,\pm 2,\ldots,. \end{cases} \quad (9)$$

The E^q in Eq. (7) are cyclic components of unit vector $\hat{\mathbf{E}}$ describing light polarization,[5,43] whilst $G(J',J'')$ in Eqs. (8) and (9) is the Hönl–London factor

$$G(J',J'') = (2J''+1)(C^{J'\Lambda'}_{J''\Lambda''1\Lambda'-\Lambda''})^2, \quad (10)$$

$C^{c\gamma}_{a\alpha b\beta}$ being Clebsch–Gordan coefficients.

To determine ${}^{kl}\Delta\omega_{MM'}$, one needs Stark energy expressions E^{el}_M. In the first approximation one can obtain first order Stark energies ${}^{(1)}E^{el}_M$ in a simple analytical form (the energy of $^1\Pi$ state f-sublevel is considered to be zero):

$${}^{(1)}E^{el}_M = \frac{1}{2}\Delta^J_{ef} \pm \sqrt{\frac{(\Delta^J_{ef})^2}{4} + \frac{d_p^2\mathscr{E}^2M^2}{[J(J+1)]^2}}. \quad (11)$$

It is easy to see that, as $\mathscr{E}$ increases, leading to $d_p\mathscr{E}M/[J(J+1)] \gg \Delta^J_{ef}/2$, Stark energy shifts have linear asymptotic behaviour with respect to $|\mathscr{E}M|$, see Fig. 1(b). A second order approximation in the ${}^{kl}\Delta\omega_{MM'}$ calculation takes place if one is accounting for the interaction between J' and adjacent $J'\pm 1$ excited state levels. The Stark-effect-induced energy second-order correction for a $^1\Pi$ state can be also written in analytical form, see Ref. 13. However, with $\mathscr{E}$ increasing, the second-order perturbation treatment becomes incorrect as well, and one has to solve the secular equation system[44] for the relevant Hamiltonian matrix. The analysis of such a treatment, accounting for $J\pm\Delta J$ mixing within a given vibrational state centered at the initial (J''), excited (J') and final (J_1'') rotational state of a $J''\rightarrow J'\rightarrow J_1''$ transition, will be given in Section IV.

III. EXPERIMENT

$^{23}Na^{39}K$ molecules were formed thermally in a glass cell joined to the vacuum system by means of a dry valve. The cylindrical head of the cell was made from a special alkali-resistant glass tube. An electric field was produced by applying a static voltage across a pair of round polished stainless steel parallel Stark plates located inside the cell. Altogether three cells were used, differing in diameter (d) and spacing (l) of the electrodes, namely: (1) $d=25$ mm, $l=2.9\pm0.1$ mm; (2) $d=7$ mm, $l=1.8\pm0.1$ mm; (3) $d=7$ mm, $l=1.2\pm0.1$ mm. The spacing between the electrodes was measured by means of a measuring microscope. The cells were filled with metallic potassium and sodium, via a repeated distillation process, in a weight ratio of approximately 7:3, respectively. The metal-containing reservoir was kept at stabilised temperatures between 270 °C and 320 °C. The dc voltage was kept below the threshold for electrical breakdown in the cell, which did not exceed 6 kV/cm at any of the temperatures employed.

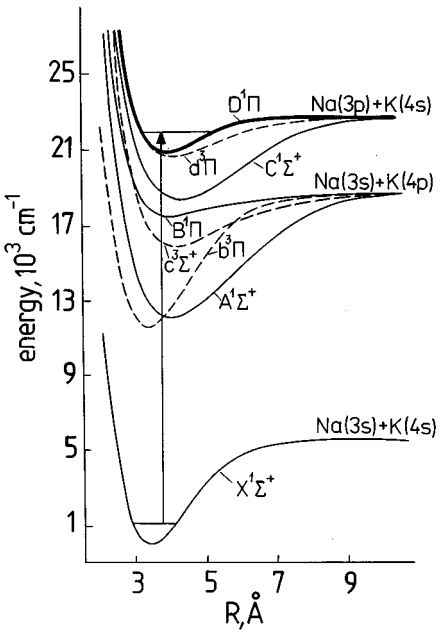

FIG. 2. Low-lying bonded terms of the NaK molecule (Ref. 25).

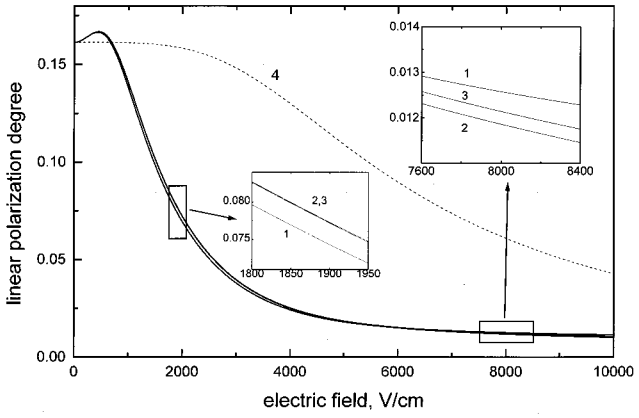

FIG. 3. Stark zero-field level-crossing signals calculated in a wide range of electric field $\mathscr{E}$ for degree of linear polarization $P(\mathscr{E})=(I_y-I_x)/(I_y+I_x)$ in ''traditional'' Stark–Hanle effect geometry ($\hat{\mathbf{E}}\perp\mathscr{E}$, observation along $\mathscr{E}$) at a transition $(J''=22)\rightarrow(J'=23)\rightarrow(J_1''=22)$. 1 — first order. 2 — Hamiltonian diagonalization, $\Delta J'=\Delta J''=\Delta J_1''=1.3$ — $\Delta J'=\Delta J''=\Delta J_1''=2$. The parameters characteristic for NaK($D^1\Pi$) state were used for simulation: $\Gamma=5\times10^7$ s^{-1} (Ref. 33), $B_v'=0.0643$ cm^{-1} $B_v''=0.0945$ cm^{-1}, $q=1.2\times10^{-5}$ cm^{-1} (Ref. 26), $d_p=7$ D (Ref. 25). Curve 4 (dashed line) refers to pure quadratic Stark effect in a hypothetic $^1\Sigma$ excited state with the same Γ and d_p values.

The linearly polarized light from a cw Ar^+-laser was used to excite $X^1\Sigma^+\rightarrow D^1\Pi$ transitions in $^{23}Na^{39}K$ molecules, see Fig. 2. Fluorescence at right angles, both to the laser beam and to the electric field $\mathscr{E}$, originating from the ca. 0.5−1.2 mm diameter laser beam excitation region, was imaged onto the entrance slit of a double monochromator with 5 Å/mm dispersion and resolved by a 1200 lines/mm grating in first diffraction order, providing an overall spectral resolution up to 0.3 Å. We restricted the observation zone to the size of ca. 1.5 mm in height, thus diminishing the possible influence of electric field inhomogeneity. The particular $D^1\Pi\rightarrow X^1\Sigma^+$ LIF progressions, originating from the definite $D^1\Pi$, v',J' states, were identified from the recorded LIF spectrum by comparison of line positions and relative intensities with the ones calculated by means of spectroscopic constants given by the authors of Ref. 26, for the transitions mentioned by them at excitation by 4765 Å and 4880 Å Ar^+-laser lines. The data from Ref. 45, considering optical depopulation of the ground $^1\Sigma^+$ state of NaK, allowed us to suppose that non-linear optical pumping effects[5,46] are negligible at the range of excitation–relaxation parameters employed. The degree of linear polarization was measured by dividing the entrance slit of the monochromator in height into two parts, placing two orthogonal polarizers in front of them. Light guides conducted fluorescence light from the two respective parts of the exit slit to the two photomultipliers, with subsequent counting of one-photon pulses from the two channels. The unpolarized LIF in the absence of an external electric field, excited by the laser light with $\hat{\mathbf{E}}$-vector set parallel to the observation direction, was used to calibrate the channels before each experiment.

In the case of optical–electric RF double resonance experiments, we used a 1–300 MHz (0.2 W, 50 Ω) Wavetek RF oscillator supply, which was connected to the same Stark plates instead of a static electric field source. A fast oscilloscope served as a 50 Ω load and as a RF output drift monitor. The resonance was measured by sweeping the frequency of the RF generator.

IV. SIMULATION OF EXPECTED SIGNALS

We will apply the developed theory to simulate the $^1\Pi$ state Stark signals in the intensity and linear polarization $P(\mathscr{E})$ of $D^1\Pi\rightarrow X^1\Sigma^+$ fluorescence. We use the dynamical parameters close to the ones which can be found in literature, namely, the dipole moment value $d_p=7$ D (following theoretical prediction in Ref. 25), the lifetime $\Gamma^{-1}=20$ ns (as determined in Ref. 33), the q-factor $q=1.2\times10^{-5}$ cm^{-1} and the rotational constant B_v values given in Ref. 26. The absolute values of d_p and q will be assumed hereafter, since their sign does not affect the calculation results.

First, we will present zero-field level-crossing signal simulations for the ''traditional'' geometry ($\hat{\mathbf{E}}\perp\mathscr{E}$, observation along $\mathscr{E}$). Figure 3 presents such calculations for the $J'=23$ level of the $D^1\Pi$ state. In the $\mathscr{E}$ range demonstrated in Fig. 3, the signal is determined by the first-order effect, the difference between the first-order approximation (curve 1) and the second-order one (curve 2) being small, yet still distinguishable. Taking into account the Stark mixing between $J\pm\Delta J$ with $\Delta J>1$ practically does not change the signal, cf. curves 2 and 3 at the insertion in Fig. 3. The monotonous behaviour of pure quadratic Stark-Hanle effect for a hypothetic $^1\Sigma$ state, supposing the same Γ, d_p and B_v' as for $^1\Pi$ state, is also presented in Fig. 3, see curve 4. A comparison of curves 1–3 and curve 4 demonstrates clearly the peculiarity of $^1\Pi$-state Stark effect, the latter possessing a small additional maximum, which appears mainly due to

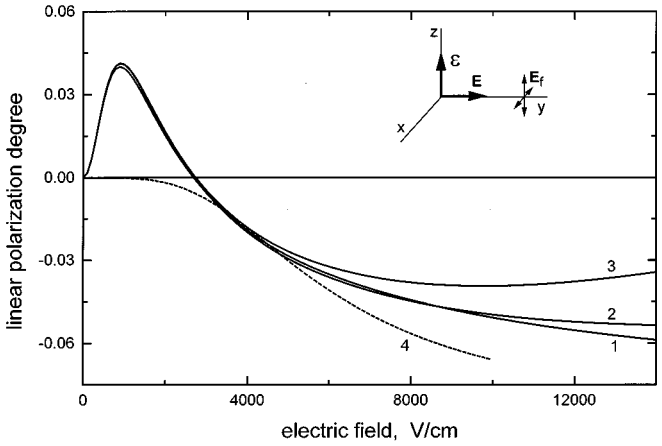

FIG. 4. Calculated $^1\Pi$ ($J'=23$) state Stark level crossing signals in degree of linear polarization $P(\mathscr{E})=(I_z-I_x)/(I_z+I_x)$ of LIF viewed from the ''end'' of the exciting light vector $\hat{\mathbf{E}}$ as shown in the setting-in. 1 — $\Delta J=0$ (linear approximation). 2 — $\Delta J=1$. 3 — $\Delta J=2$. Curve 4 represents calculated signal for a hypothetic $^1\Sigma$ state. Parameters are the same as in Fig. 3.

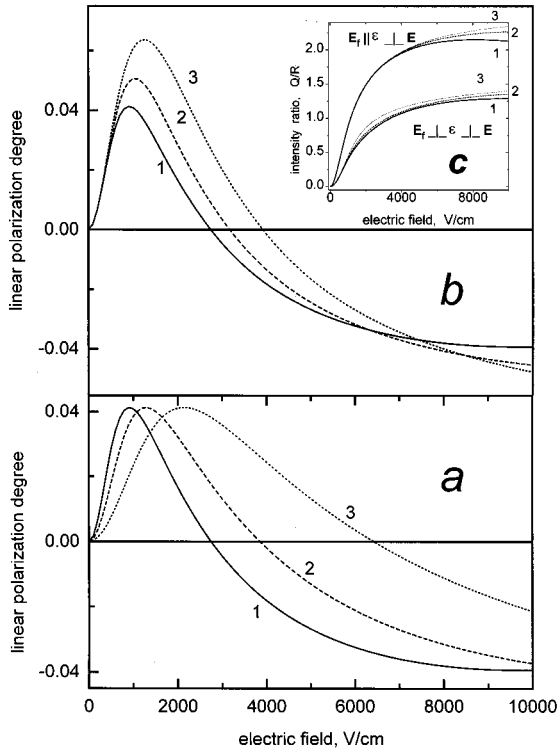

FIG. 5. (a) Simulations of Stark level crossing signals in polarization of LIF from $^1\Pi$ ($J'=23$), assuming the same $q=1.2\times10^{-5}$ cm^{-1} value and different permanent electric dipole moment values: 1 — $d_p=7$ D, 2 — $d_p=5$ D, 3 — $d_p=3$ D. (b) The same signals for different q and d_p values in condition of the constant q/d_p ratio. 1 — $q=1.2\times10^{-5}$ cm^{-1}, $d_p=7$ D. 2—$q=0.857\times10^{-5}$ cm^{-1}, $d_p=5$ D. 3—$q=0.514\times10^{-5}$ cm^{-1}, $d_p=3$ D. (c) Correspondent intensity ratios $I_Q/I_{P,R}$ calculated for the same parameters at two orthogonal fluorescence polarization directions. Calculations are performed with fixed relaxation rate $\Gamma=5\times10^7$ s^{-1}. Geometry and other parameters are the same as in Fig. 4.

the competition between the M-dependent Stark induced $e-f$ mixing and the destruction of coherence among M-sublevels.

This peculiarity in $P(\mathscr{E})$ is more pronounced at another geometry, when fluorescence is observed ''from the end'' of $\hat{\mathbf{E}}$-vector, $\hat{\mathbf{E}}\perp\mathscr{E}$ (see Fig. 4). Both first-order ($\Delta J=0$, curve 1) and second-order ($\Delta J=1$, curve 2) approximations are insufficient to describe with adequate accuracy the polarization in the coherence destruction region. This can be seen from comparison with curve 3 obtained via Hamiltonian diagonalization accounting for Stark mixing between $J\pm\Delta J$ with $\Delta J=2$; accounting for $\Delta J>2$ practically does not affect the result. We will further exploit the geometry shown in Fig. 4, performing ($\Delta J=2$)-approximation in the calculations of Stark effect signals.

Let us now investigate the sensitivity of the signal presented in Fig. 4 to the variations of the main parameters of the $^1\Pi$ state, namely to the permanent electric dipole moment d_p, Λ-doubling constant q and relaxation rate Γ values. The results are presented in Figs. 5 and 6. Figure 5(a) demonstrates a polarization signal simulation at d_p values taken as 3 D, 5 D and 7 D, when all other parameters remained unchanged. In Fig. 5(b), the d_p and q values have been varied simultaneously, whereas their ratio was maintained constant. It can be seen from comparison between Figs. 5(a) and 5(b) that the peak amplitude is uniquely determined by the q value, whilst the position of the peak in $\mathscr{E}$-scale and the slope of the growing part are mainly determined by the d_p value. This allows one to determine simultaneously both d_p and q values from one fit, provided that Γ is known. The situation is quite different for the intensity ratios $I_Q/I_{P,R}$ of Stark induced ''forbidden'' line I_Q to the ''parent'' line $I_{P,R}$, see Fig. 5(c). Indeed, the respective curves in Fig. 5(c) undergo minor changes at different d_p and q used in calculations presented in Figs. 5(a) and 5(b), if the q/d_p ratio remains unchanged, thus only this ratio can be

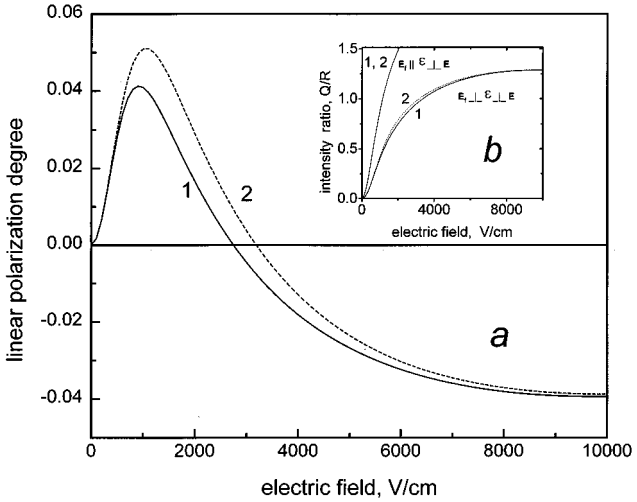

FIG. 6. Simulations of Stark level crossing signals in polarization of LIF from $^1\Pi$ ($J'=23$), and intensity ratio I_Q/I_R, assuming different Γ values. 1 — $\Gamma=5\times10^7$ s^{-1}. 2 — $\Gamma=7\times10^7$ s^{-1}. Calculations are performed with $q=1.2\times10^{-5}$ cm^{-1}, $d_p=7$ D. (a) — LIF polarization. (b) — Intensity ratios.

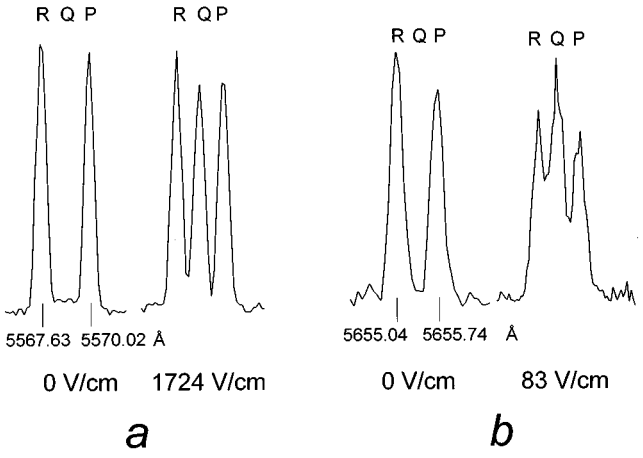

FIG. 7. Effect of electric field on spectrally resolved LIF signal for NaK $D^1\Pi \rightarrow X^1\Sigma^+$ system. (a) transition $(v''=1,J''=22)\rightarrow(v'=7,J'=23)\rightarrow(v_1''=24,J_1''=22$ and $24)$; 4880 Å excitation. (b) transition $(v''=0,J''=8)\rightarrow(v'=12,J'=7)\rightarrow(v_1''=31,J_1''=6$ and $8)$; 4765 Å excitation.

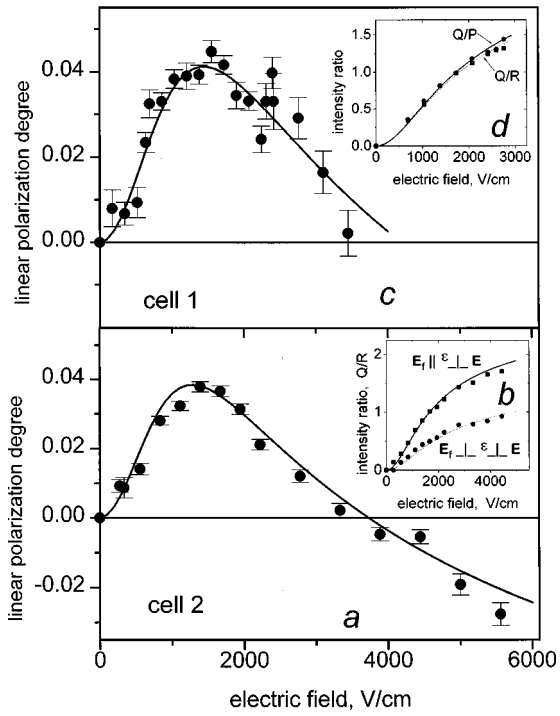

FIG. 8. Linear polarization degree and intensity ratios measured in LIF from NaK $(D^1\Pi)$ state with $v'=7,J'=23$. (a), (c) — electric field dependence of the polarization degree obtained on $R(22)$ component. (b), (d) — electric field dependence of intensity ratios I_Q/I_P or I_Q/I_R. Results are obtained in different cells at geometry depicted in Fig. 4, dots are the measured values, the lines refer to the calculations at fitted parameters.

determined from the fitting. Figure 6 demonstrates the sensitivity of the signals under discussion with respect to the variation in the relaxation rate Γ. As expected, the changes of polarization signal $P(\mathscr{E})$ with Γ are quite similar to respective $P(\mathscr{E})$ changes with q (cf. Fig. 6(a) and Fig. 5(b)). In contrast, the intensity ratios are almost insensitive to Γ variations, especially for the $\mathscr{E}\|\hat{\mathbf{E}}_\mathbf{f}$ geometry (see curves 1 and 2 in Fig. 6(b)).

V. MEASUREMENTS AND RESULTS

NaK $D^1\Pi$ state electric dipole moment and Λ-splitting measurements have been carried out by the following methods:

(i) by recording spectrally resolved LIF and measuring the intensity ratio between ''forbidden'' and allowed (''parent'') lines as a function of static voltage;
(ii) by measuring the variation of the degree of linear polarization of the ''parent'' line with variation in the static voltage;
(iii) by measuring the electric RF – optical double resonance Λ-doublet signal from the ''forbidden'' line intensity dependence on RF field frequency.

A. Intensity ratios

Figure 7 demonstrates the effect of static electric field on the spectrally resolved LIF leading to the appearance of forbidden Q line due to $e-f$ mixing. Since the effect is mainly governed by the $\mathscr{E}d_p/\Delta_{ef}^J$ ratio, one needs a larger electric field strength to observe the Q-lines originating from $v'=7,J'=23$ than from the $v'=12,J'=7$ state. The (P,Q,R)-triplet component separation for the latter case, being ca. 0.3 Å, is on the edge of the spectral resolution of the monochromator used.

A fitting procedure employing three Gaussians was used to obtain ''forbidden''/''parent'' line ratio $I_Q/I_{P,R}$. The intensity ratios $I_Q/I_{P,R}$, obtained in different cells (see Section III) and experimental geometries, are shown as insets in Figs.

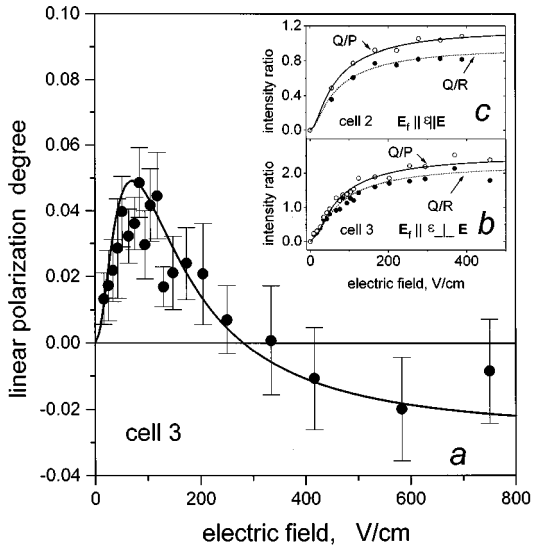

FIG. 9. Linear polarization degree and intensity ratios measured in LIF from NaK $(D^1\Pi)$, $v'=12,J'=7$. (a) — electric field dependence of polarization degree obtained on $P(8)$ component. (b), (c) — electric field dependence of intensity ratios I_Q/I_P and I_Q/I_R. Data for (a), (b) are obtained at geometry depicted in Fig. 4, whereas for (c) we used $\hat{\mathbf{E}}\|\mathscr{E}$. Dots are the measured values, full lines refer to the calculations with fitted parameters.

TABLE I. Experimental values of permanent electric dipole moment d_p and Λ – doubling constant q for NaK $(D^1\Pi, v', J')$. Values d_p^{th} are *ab initio* calculations (Ref. 25) averaged for a particular v'.

v'	J'	q, 10^{-5} cm^{-1}	d_p, Debye	d_p^{th} Debye
7	23	1.65 ± 0.20[a]	6.4 ± 0.8[a]	7.1
		1.42 ± 0.07[b]	5.9 ± 0.9[c]	
12	7	1.10 ± 0.20[a]	4.5 ± 0.8[a]	6.5
		1.03 ± 0.08[b]	4.8 ± 0.9[c]	

[a]Values determined from two-parameter fitting of LIF polarization $\mathscr{E}$-dependencies.
[b]Values determined directly from RF-optical double resonance.
[c]Values determined using q/d_p obtained from the $\mathscr{E}$-dependence of $I_Q/I_{P,R}$ and q obtained from RF-optical double resonance.

8 and 9. Least-square data processing yielded q/d_p ratios. The averaged values are $(2.40\pm0.25)\times10^{-6}$ cm$^{-1}/D$ for $v'=7, J'=23$ and $(2.10\pm0.20)\times10^{-6}$ cm$^{-1}/D$ for $v'=12, J'=7$ state. The q/d_p systematic errors are most likely attributable to uncertainties in Stark plate separation. For instance, the curves in Figs. 9(b), 9(c) demonstrate the $\mathscr{E}$-dependences of I_Q/I_P and I_Q/I_R, which are registered for two different cells and different exciting light vector directions, $\hat{\mathbf{E}}\|\mathscr{E}$ or $\hat{\mathbf{E}}\|\mathscr{E}$, with fluorescence light vector $\hat{\mathbf{E}}_\mathbf{f}\|\mathscr{E}$ in both cases. The one-parameter (q/d_p) least-square routine yields the following constant ratios: $q/d_p=1.9\times10^{-6}$ cm$^{-1}/D$ for Fig. 9(b) and $q/d_p=2.3\times10^{-6}$cm$^{-1}/D$ for Fig. 9(c), the discrepancy reflecting both statistical and systematic errors.

B. Polarization measurements

1. Results for the $D^1\Pi(v'=7, J'=23)$ state

Experimentally measured electric field dependencies of the polarization degree are presented in Fig. 8. The results are obtained in two different cells (see Section III), using the most favourable geometry when LIF is viewed from the ''end'' of exciting light vector $\hat{\mathbf{E}}\perp\mathscr{E}$, as depicted in Fig. 4. The data fitting was realized by accounting for Stark interaction among five rotational states $J, J\pm1, J\pm2$ for all J'', J' and J_1'' involved in the transition. The best-fit constants q and d_p, obtained from a two-parameter weighted least-square routine, yield the values in question. Cell 1 yields $q=1.6\times10^{-5}$ cm^{-1} and $d_p=6.3$ D, whilst cell 2 yields $q=1.7\times10^{-5}$ cm^{-1} and $d_p=6.5$ D. Cell 2 allowed us to achieve higher electric field intensities (up to 5.6 kV/cm) owing to the special working of Stark plates surface and edges in order to avoid sparking; the conditions were more favourable also because of lower cell temperatures (ca. 270 °C). On the other hand, the results for cell 2 may have a larger systematic error because of smaller plate separation. Evaluation of the possible contribution of both statistical and systematic errors for different cells enabled us to take $d_p=(6.4\pm0.8)$ D and $q=(1.65\pm0.2)\times10^{-5}$ cm^{-1} as the averaged permanent electric dipole moment and q-factor values, see Table I. As it follows from the simulations presented in Figs. 5 and 6, the Λ-doubling constant q obtained from the fit seems to be more subject to the systematic error in absolute polarization values, which can arise, say, from even slight inaccuracies in the calibration of channels and in accounting for background signal, as well as any possible uncertainty in the relaxation constant Γ value.

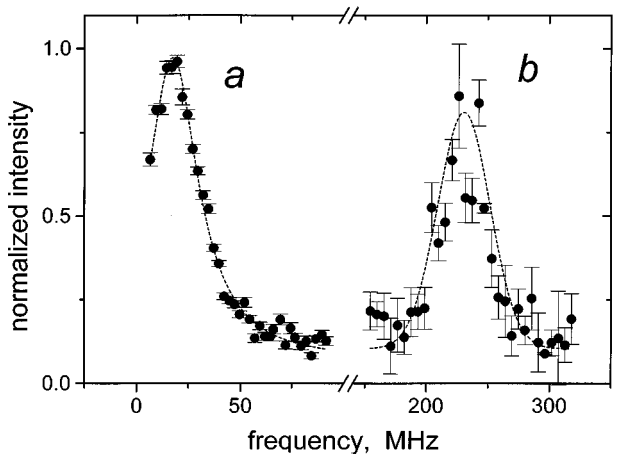

FIG. 10. RF-optical double resonance signals. (a) For NaK $D^1\Pi$ $v'=12, J'=7$ state. (b) For NaK $D^1\Pi$ $v'=7, J'=23$ state.

2. Results for the $D^1\Pi(v'=12, J'=7)$ state

Measurements for this state were much more complicated because of the small spectral separation between the triplet components (see Fig. 7(b)), requiring narrow spectrometer slits to maintain necessary resolution. This leads to considerably larger errors, both statistical and systematic, in polarization measurements (see Fig. 9(a)). The most favourable conditions were achieved using cell 3 (see Section III). $P(\mathscr{E})$ was registered in P-transitions $(J'=7)\rightarrow(J_1''=8)$ because of better spectral separation. In spite of wide statistical scatter in the results, we have accomplished direct least-square two-parameter fitting, which yielded the values $d_p=4.5\pm0.8$ D and $q=(1.1\pm0.2)\times10^{-5}$ cm^{-1}, see Table I. The large inaccuracy in the q value accounts for the uncertainty in relaxation rate Γ for this state. We supposed Γ to be 5×10^7 s^{-1}, that is the same as for the $v'=7, J'=23$ state.[33]

C. Electric RF – optical double resonance

Since the routine based on both d_p and Δ_{ef}^J variation in the fitting of the measured $P(\mathscr{E})$ signal is very sensitive to inaccuracies in absolute $P(\mathscr{E})$ measurements, as well as to Γ values (see Figs. 5 and 6), it seemed important to exploit a method allowing direct Δ_{ef}^J measurement in some independent experiment. For this purpose we have employed the electric RF – optical double resonance method. In order to increase the RF field amplitude $\mathscr{E}_{\mathrm{RF}}^o$, the measurements were carried out at a Stark-plate separation of 0.85 ± 0.05 mm. The RF field voltage enabled us to produce $\mathscr{E}_{\mathrm{RF}}^o\lesssim$ 20 V/cm. In order to diminish LIF intensity drift during signal accumulation the normalised difference $(I_F-I_{F_o})/I_{F_o}$ was considered to be a result of a single measurement, that is the difference

between intensity at current frequency F and at some reference frequency F_o. The signal accumulation time varied from 10 minutes to 1 hour.

1. Results for the $D^1\Pi_u, v'=7, J'=23$ state

Figure 10(b) (dots) presents experimental data obtained by registering the intensity of a ''forbidden'' Q-line as dependent on the RF electric field frequency, demonstrating resonance intensity increase, with a maximum near 230 MHz. Although the resonance signal width exceeded the one expected from the natural broadening, probably possessing some structure, we assumed that the signal is reliable enough to determine the e/f separation Δ^J_{ef}, yielding $q=(1.42\pm0.07)\times10^{-5}$ cm^{-1} as an averaged value. This makes it possible to determine the permanent electric dipole moment d_p in question, using q/d_p values presented in Section VA, as $d_p=5.9\pm0.9$ D.

2. Results for the $D^1\Pi_u, v'=12, J'=7$ state

Figure 10(a) presents the experimental data (dots) demonstrating the RF field frequency dependence of the ''forbidden'' Q-line intensity in $(J''=8)\rightarrow(J'=7)\rightarrow(J''_1=7)$ transition. The average of q over a number of experiments is $q=(1.03\pm0.08)\times10^{-5}$ cm^{-1}. Taken together with q/d_p obtained from intensity ratios, see Section VA, the dipole moment value is $d_p=(4.8\pm0.9)$ D, where the estimated relative error consists of 10% assigned to q/d fitting and 8% assigned to Δ^J_{ef} uncertainty.

VI. DISCUSSION AND CONCLUSIONS

A. Method

Investigation of permanent electric dipole moments is not an easy matter for short-lived excited molecular states with large rotational numbers ($J\gg1$). Let us compare the two more or less independent methods exploited in the present work. Both methods are based on analyzing Stark effect induced changes in fluorescence, which are caused predominately by $e-f$ mixing within the same rotational state, which, in turn, is governed mainly by dipole moments (d_p), Λ-splittings (Δ^J_{ef} or q-factors) and relaxation rates (Γ).

(i) *$\mathscr{E}$-dependence of linear polarization degree $P(\mathscr{E})$.* In the most favourable experimental geometry the $P(\mathscr{E})$ signal is characteristic enough to obtain both q and d_p from the fitting. This demands high accuracy in measuring $P(\mathscr{E})$ and precise knowledge of the relaxation rate Γ.

(ii) *RF – optical double resonance along with $\mathscr{E}$-dependence of intensity ratios* of ''forbidden'' – to – ''parents'' lines in LIF triplet exhibit an alternative method. In this case the RF resonance yields directly the Λ-doubling splitting Δ^J_{ef} whilst the processing of relative intensity data yields Δ^J_{ef}/d_p, the latter procedure being weakly dependent on Γ. Thus, the accuracy of d_p values in question, obtained by this method is only slightly affected by the accuracy of relaxation rate Γ. A crude estimate of Γ gained from the width of the RF–optical double resonance may even work to obtain reliable d_p values without any previous knowledge of molecular lifetime.

The developed theoretical description (Section II) and simulations of expected signals (Section IV) allowed us to conclude that, even though the main Stark features arise from the 1st order effect, in order to avoid possible inaccuracies in the case when the Stark energy is not too small in comparison with rotational splitting (i.e., in case of not too small $d_p\mathscr{E}/(B'_vJ')$), it is necessary, for both methods (i) and (ii), to consider Stark interaction with no less than four neighbouring rotational levels, both in excited and ground (initial and final) states.

Dipole moments and Λ-splittings. The dipole moments determined seem to be reliable, in particular since there is good agreement between the results gained from two independent methods. As for the absolute d_p values, they can be considered as very large when compared to typical dipole moment values which had been measured for diatomic molecules.[13,47] Let us compare the measured d_p values with theoretical quantities given by Stevens, Konowalow and Ratcliff.[25] In order to pass from *ab initio* $d^{th}_p(R)$ dependence presented in Ref. 25 to the predicted d_p values for particular v',J' states, we have used the averaging routine based on either *ab initio* potentials,[25] or RKR potentials[26] for the NaK $D^1\Pi$ state. The results differ by no more than 1%, yielding the following predicted $d^{th}_p(v',J')$ values for the states under study: $d^{th}_p(7,23)=7.1$ D and $d^{th}_p(12,7)=6.5$ D, see Table I.

As follows from Table I, the measured d_p value for the $v'=12,J'=7$ state is smaller than for the $v'=7,J'=23$, being also markedly smaller than the theoretically predicted value. As is well known,[26,31,32] levels belonging to the NaK $D^1\Pi$ state are perturbed, at least to some extent, by the close lying $d^3\Pi$ state. Basing on Ref. 26, the level $v'=7,J'=23$ can be considered as almost unperturbed, whereas the level $v'=12,J'=7$ is shifted to $\Delta E=0.468$ cm^{-1} with respect to the deperturbed position. Using the calculated difference of deperturbed $D^1\Pi$ $(v'=12)$ and $d^3\Pi$ $(v'=13)$ terms[31] with $J'=7$, being $E_{^3\Pi}-E_{^1\Pi}=3.87$cm^{-1}, one can get the estimation for the squared state mixing coefficient $C^2_{^3\Pi}=\Delta E/(E_{^3\Pi}-E_{^1\Pi})\cong0.13$. This creates a reduction in pure singlet character of the state to $C^2_{^1\Pi}=1-C^2_{^3\Pi}\cong0.87$ and allows one to estimate the relative change in the $D^1\Pi$ $(v'=12,J'=7)$ state electric dipole moment, which arises due to singlet–triplet coupling, as $C^2_{^1\Pi}+C^2_{^3\Pi}(d^{^3\Pi}_p/d^{^1\Pi}_p)$, $d^{^3\Pi}_p$ and $d^{^1\Pi}_p$ being unperturbed dipole moments. The averaging of the *ab initio* calculations[25] for the $d^3\Pi, v'=13$ state yields $d^{^3\Pi}_p\cong-0.7$ D, which is opposite in sign from $d^{^1\Pi}_p$. As a result, the experimentally measured d_p value for $(D^1\Pi, v'=12,J'=7)$ is expected to be ca. 15% smaller than would be anticipated for the unperturbed state. It is thus not excluded that the difference between d_p values obtained for the two states, see Table I, reflects the role of perturbations.

Indeed, the relative difference between the measured d_p values for $v'=7,J'=23$ and $v'=12,J'=7$ is ca. 20% – 25%, which does not contradict the above estimation. Hence, the experimentally measured d_p values do not disprove the *ab initio* calculation in Ref. 25, accounting for the fact that the deperturbed quantities have been calculated.

Regarding the Λ-doubling factor q, it can be noted that its tendency to be smaller for $v'=12,J'=7$ level, corresponds to what can be expected due to the perturbation, allowing one to estimate a ca. 13% diminution from the following considerations. Although the singlet–triplet $D^1\Pi-d^3\Pi$ interaction does not change the Λ-doubling splitting directly since e and f components of the $D^1\Pi$ state are perturbed by the two Λ-doublet substates of the $d^3\Pi$ state to about the same amount, this singlet–triplet interaction diminishes the singlet character of the perturbed state as $C^2_{^1\Pi}$ Hence, the matrix element of electronic–rotational interaction with the remote singlet Σ states, giving rise to Λ-doubling in the $D^1\Pi$ state, has to be $C_{^1\Pi}\langle D^1\Pi|L^{\pm}|^1\Sigma\rangle$, since the matrix elements between the states having a different multiplicity vanish. The q value for NaK ($D^1\Pi$) presented in Ref. 26 has been obtained from conventional spectroscopic analysis as $q_v=q_0-q_1(v+1/2)=1.16\times10^{-5}-1.5\times10^{-7}(v+1/2)$ cm^{-1}. The RF – optical double resonance signal for NaK ($D^1\Pi,v'=7,J'=5$) can be found in Ref. 16, yielding $q=1.5\times10^{-5}$ cm^{-1}. Thus, the q-factor values presented in Table I do not disagree much with the previous data. The Λ-doubling constant for $D^1\Pi$ state can be estimated from the well-known relation: $q\approx 4B_e^2/\nu(\Pi,\Sigma)$, where $\nu(\Pi,\Sigma)$ is the difference between the electronic term values $T_\Pi-T_\Sigma$. Then, assuming that $D^1\Pi$ state Λ-doubling arises from the interaction with low-lying $C^1\Sigma$ and $A^1\Sigma$ states, one gets $q\approx1.2\times10^{-5}$ cm^{-1}.

As mentioned above, the experimental data on excited-state electric dipole moments of any alkali diatomic are extremely scanty. The authors of Ref. 24 present d_p values varying from 2.4 to 2.1 D for the NaK $B^1\Pi$ state with v' equaling 1, 5, 10 and 14. The d_p values are smaller than the ones predicted from *ab initio* calculations by Stevens and co-authors,[25] which, according to averaging as mentioned above, range from $d_p^{th}=4.5$ D for $v'=1$ to $d_p^{th}=2.8$ D for $v'=14$. It can be noted however that there are some contradictions in q-factors determined in the measurements,[24] presenting, for instance, the absolute values $q=0.65\times10^{-6}$ cm^{-1} for $v'=1$ and $q=1.77\times10^{-6}$ cm^{-1} for $v'=5$. These quantities disagree with the respective values $q=2.08\times10^{-6}$ cm^{-1} and $q=2.36\times10^{-6}$ cm^{-1} obtained for corresponding v' by Baba, Tanaka and Kato[48] using Doppler-free polarization spectroscopy. In order to obtain the same q/d_p ratio as presented in Ref. 24 with q values from Ref. 48 instead of the ones given in Ref. 24, the d_p for $v'=5$ should be increased from 2.4 D to 3.2 D, the latter being not far from the averaged calculated value $d_p^{th}(v'=5)=3.9$ D.[25] The results given in Ref. 24 for the $v'=1$ level of NaK $B^1\Pi$ seem strange since it is hard to imagine so dramatic a change in q (being 3 times smaller than for $v'=5$), whilst dipole moments remain unchanged, see Table III in Ref. 24.

In conclusion, the measurements constituted in the present work confirm the existence of a large permanent electric dipole moment in the NaK $D^1\Pi$ state. It is of importance to strive to refine the experimental d_p values. Besides increasing the accuracy of measurements and extending the number of vibrational states involved in the investigation, there is reason to believe that further progress is connected with accounting for intramolecular perturbation, the most important of which might involve the simultaneous effects of hyperfine structure and $d^3\Pi$ – $D^1\Pi$ interaction.

ACKNOWLEDGMENTS

This work was supported by Long Term Grant LJ7100 (1995) in the frame of the Joint Programme of the Government of Latvia and the International Science Foundation. Four of us (M.T., M.A., I.K., and R.F.) are grateful for the support from the Latvian Science Council (Grant No. 93.256), as well as for the support from the European Commission in the frame of PECO Human Capital & Mobility (Networks) programme, Contract No. ERBCIPDCT940633. One of us (A.V.S.) is grateful for the support from Russian Foundation for Basic Research (Grant No. 93-03-18059). It is our pleasant duty to thank Professor Richard N. Zare for fruitful recommendations. We are also indebted to Dr. Yelena Pazyuk and Professor Pawel Kowalczyk for useful discussions. We are grateful to Vitauts Boreishis for his assistance in experiments, as well as to Dr. Henrik Rudolph and Dr. Henk Dijkerman for granting the RF oscillator.

[1] W. Hanle, Z. Phys. **5**, 246 (1926).
[2] W. Hanle, Z. Phys. **30**, 93 (1924).
[3] E. B. Alexandrov, M. P. Chaika, and G. I. Khvostenko, *Interference of Atomic States* (Springer, New York, 1993).
[4] G. Moruzzi and F. Strumia, *Hanle Effect and Level-Crossing Spectroscopy* (Plenum, New York, 1991).
[5] M. Auzinsh and R. Ferber, *Optical Polarization of Molecules* (Cambridge University Press, Cambridge, 1995).
[6] R. N. Zare, J. Chem. Phys. **45**, 4510 (1966).
[7] A. Khadjavi, A. Lurio, and W. Happer, Phys. Rev. **167**, 128 (1968).
[8] N. D. Bhaskar and A. Lurio, Phys. Rev. A **10**, 1685 (1974).
[9] S. J. Silvers, T. H. Bergeman, and W. Klemperer, J. Chem. Phys. **52**, 4385 (1970).
[10] F. W. Dalby, M. Broyer, and J. C. Lehmann, Colloid Int. CNRS **217**, 227 (1974).
[11] G. Dohnt, A. Hese, A. Renn, and H. S. Schweda, Chem. Phys. **42**, 183 (1979).
[12] C. H. Townes and A. L. Schawlow, *Microwave Spectroscopy* (McGraw–Hill, New York, 1955).
[13] M. Mizushima, *Theory of Rotating Diatomic Molecules* (Wiley, New York, 1975).
[14] G. Herzberg, *Molecular Spectra and Molecular Structure. I. Spectra of Diatomic Molecules* (Van Nostrand, Princeton, 1957).
[15] H. Lefebvre-Brion and R. W. Field, *Perturbations in the Spectra of Diatomic Molecules* (Academic, New York, 1986).
[16] R. E. Drullinger, M. M. Hessel, and E. W. Smith, in *Laser Spectroscopy*, edited by S. Haroche *et al.* (Springer, Berlin, 1975), p. 91.
[17] C. A. Moore, G. P. Davis, and R. A. Gottscho, Phys. Rev. Lett. **52**, 538 (1984).
[18] M. L. Mandich, C. E. Gaebe, and R. A. Gottscho, J. Chem. Phys. **83**, 3349 (1985).
[19] R. A. Gottscho, Phys. Rev. A **36**, 2233 (1987).
[20] J. Derouard and N. Sadeghi, Opt. Commun. **57**, 239 (1986).

[21] H. Debontride, J. Derouard, and N. Sadeghi, Ann. Phys. **13**, 97 (1988).
[22] M. H. Alexander, J. Chem. Phys. **83**, 3340 (1985).
[23] J. Derouard and M. H. Alexander, J. Chem. Phys. **85**, 134 (1986).
[24] J. Derouard, H. Debontride, T. D. Nguyen, and N. Sadeghi, J. Chem. Phys. **90**, 5936 (1989).
[25] W. J. Stevens, D. D. Konowalow, and L. B. Ratcliff, J. Chem. Phys. **80**, 1215 (1984).
[26] M. M. Hessel and S. Giraud-Cotton, NaK revisited: The ground $^1\Sigma$ and $D^1\Pi$ states (unpublished, preprint, 1980).
[27] D. Eisel, D. Zevgolis, and W. Demtröder, J. Chem. Phys. **71**, 2005 (1979).
[28] E. J. Breford and F. Engelke, Chem. Phys. Lett. **53**, 282 (1978).
[29] E. J. Breford and F. Engelke, J. Chem. Phys. **71**, 1994 (1979).
[30] H. Katô and C. Noda, J. Chem. Phys. **73**, 4940 (1980).
[31] P. Kowalczyk, J. Mol. Spectrosc. **136**, 1 (1989).
[32] A. J. Ross, C. Effantin, J. d'Incan, and R. F. Barrow, J. Phys. B **19**, 1449 (1986).
[33] J. Pfaff, M. Stock, and D. Zevgolis, Chem. Phys. Lett. **65**, 310 (1979).
[34] R. W. Field and T. H. Bergeman, J. Chem. Phys. **54**, 2936 (1971).
[35] T. J. Scholl, R. Cameron, S. D. Rosner, and R. A. Holt, Can. J. Phys. **73**, 101 (1995).
[36] B. Friedrich and D. R. Herschbach, Nature (London) **353**, 412 (1991).
[37] C. Cohen-Tannoudji, Ann. Phys. **7**, 423 (1962).
[38] C. Cohen-Tannoudji, Ann. Phys. **7**, 469 (1962).
[39] K. Blum, *Density Matrix. Theory and Applications* (Plenum, New York, 1981).
[40] A. R. Edmonds, *Angular Momentum in Quantum Mechanics* (Princeton University Press, Princeton, New Jersey, 1974).
[41] R. N. Zare, *Angular Momentum* (Wiley, New York, 1988).
[42] I. I. Sobelman, *Atomic Spectra and Radiative Transitions* (Springer, Berlin, 1992).
[43] D. A. Varshalovich, A. N. Moskalev, and V. K. Khersonskii, *Quantum Theory of Angular Momentum* (World Scientific, Singapore, 1988).
[44] I. Rø egger, J. Phys. B **4**, 168 (1971).
[45] M. P. Auzinsh, R. S. Ferber, Ya. A. Harya, and I. Ya. Pirags, Chem. Phys. Lett. **124**, 116 (1986).
[46] R. E. Drullinger and R. N. Zare, J. Chem. Phys. **51**, 5532 (1969).
[47] K. P. Huber and G. Herzberg, *Molecular Spectra and Molecular Structure. IV. Constants of Diatomic Molecules* (Van Nostrand, New York, 1979).
[48] M. Baba, S. Tanaka, and H. Kato, J. Chem. Phys. **89**, 7049 (1989).